Bitlis Eren Üniversitesi Fen Bilimleri Dergisi
BİTLİS EREN UNIVERSITY JOURNAL OF SCIENCE
ISSN: 2147-3129/e-ISSN: 2147-3188
VOLUME: 12 NO: 4 PAGE: 941-958 YEAR: 2023
DOI:10.17798/bitlisfen.1264165

Design and Performance Analysis of an Air-Based Photovoltaic/Thermal Collector in Winter

Özer KESTANE[1*], Koray ÜLGEN[2]

[1]*Computer Programming Program, İzmir Vocational School, Dokuz Eylül University, İzmir, Turkiye*
[2]*Solar Energy Institute, Ege University, Izmir,Turkiye*
(ORCID: 0000-0001-6092-2881) (ORCID: 0000-0002-9560-1727)

Keywords: Photovoltaic, Solar air collector, PV/T system, Energy analysis, PV/T collector, Thermal energy.

Abstract

The most basic requirements of the facilities in which we spend nearly all of our time are for electricity and heat. It is critical, especially in cold climate regions, that both electrical energy and heating energy needs are met by the same system. The use of photovoltaic (PV) energy is rapidly expanding. Photovoltaic panels can convert solar energy into electrical energy with less than 20% efficiency. Solar energy applications include photovoltaic-thermal (PV/T) collectors that can be installed on building facades or used as building envelopes. Solar energy is used to generate both electric and thermal energy needs with this collector. Off-grid photovoltaic panels and some types of flat-plate solar air collectors have been considered in our work. An experimental setup and a measurement system have been constructed to investigate the behavior of the air-based photovoltaic-thermal collector. This measurement system, sensors that collect data, and a data storage unit that can communicate temperature, humidity, and radiation data to the computer at the specified frequency comprise the experimental setup. The efficiencies of the PV and the solar air collector were calculated individually to estimate the performance of the air-based PV/T collector. Calculation criteria and a model have been developed to determine the performance of this collector. The problem was viewed as time-dependent under irregular settings when developing this model. The theoretical analytical model developed to determine the performance of the air-based PV/T collector was evaluated using Izmir's, a city in the west of Türkiye, winter climatic conditions. As a result of the studies carried out to determine the experimental performance of the PV/T air collector developed within the scope of the study, the thermal efficiency of the system reached up to 35% and the electrical efficiency reached 19% during the winter months. As a result of comparing the results obtained from theoretical and experimental studies, max. It has been determined that there is an error of 0.12%.

Nomenclature

A	Area [m]
C_p	Specific heat [kJkg^{-1}K^{-1}]
h	Heat transfer coefficient [Wm^{-2}K$^{-1]}$
I	Solar Radiation [Wm^{-2}]
L	Thickness [m]
m	Air mass [kgs^{-1}]
q, Q	Thermal Heat [kJ, W]
T	Temperature [°C, K]
t	time [h]

Greek letter

η	Efficiency [%]
λ	Thermal conductivity [Wm^{-1}K^{-1}]
α	Absorptivity [-]
τ	Transmission [-]

*Corresponding author: ozer.kestane@deu.edu.tr
Received: 12.03.2023, Accepted: 09.10.2023

Subscripts

β	Tilt	PV	Photovoltaic
a	Ambient	rad	Radiation
b	Bottom	ref	Reference
c	Cell	t	Top
conv	Convective	T	Total
f	Fluid	ted	Tedlar
g	Glass	th	Thermal

1. Introduction

PV/T systems have been created in many forms and structures depending on the intended purpose of reducing temperature buildup in solar cells [1]–[4][. PV/T air collector systems, which can be integrated into building solar façades or used as building shells, are a novel type of solar application. In general, the goal of these applications is to create both electrical and thermal energy from solar energy while also meeting the energy demand of buildings [5]–[9].

Solar cells convert some of the solar energy they absorb into electrical energy, but the majority of it turns into heat energy, increasing cell temperature and lowering electrical efficiency. The output power and system efficiency of the solar cells can be enhanced during this photovoltaic conversion by cooling them by removing heat from the absorber surface and the cells using a carrier fluid. In most solar hot water preparation systems, water is employed as the fluid in collectors. To improve the efficiency of the PV/T system, phase-shifting materials capable of operating at low temperatures can be used [10]–[14].

In addition to generating electricity, these double-acting systems can produce hot water or hot air and, alternatively, use it for residential hot water and direct space heating. The use of direct ambient air as a fluid for room heating significantly improves the system's overall efficiency. Furthermore, the heated air from the PV/T collector can be provided to the building's ventilation system as pre-heated fresh air. The creation of these façade-integrated systems, which will be installed on buildings' south, southwest, and west facades, would significantly cut energy consumption. The hot air from the PV/T air collector can be used to heat the building [15], [16].

The number of publications on conventional thermal system design and thermal efficiency modelling is greater than the number of publications on combined solar cell-thermal collector design. The Hottel-Whillier model, established in 1958, is the most well-known modelling method. Later, as dynamic modelling of thermal collectors gained popularity, this was investigated. Klein et al. conducted a study of three distinct dynamic models. [17].

According to the findings, the dynamic impacts cancel each other out over the day. Suzuki and Kitamura's [18] theoretical and experimental work on hybrid PV/T systems provides the main ideas of these systems with the results of employing water or air as a cooling fluid.

The aim of the systems developed within this logic is to provide a combined (hybrid) solution by providing both heat and electricity generation together in the same area. Today, PV/T systems, which produce electricity and heat together, are mostly focused on the systems that are introduced as a result of the integration of solar collectors and solar cells. Today, solar energy is used in two ways: thermal solar systems, in which solar radiation from the earth is converted to heat, and photovoltaic (PV) systems, in which solar energy is transformed into electrical energy. Thermal solar systems are utilized for a variety of purposes, including water heating, space heating, and mechanical power generation. Photovoltaic systems convert solar radiation directly to electrical energy and are utilized to address the electrical energy demands of houses and commercial operations.

Figure 1 shows the comparison of the PV module used in electricity generation and the PV system resulting from the integrated thermal system used in heat generation.

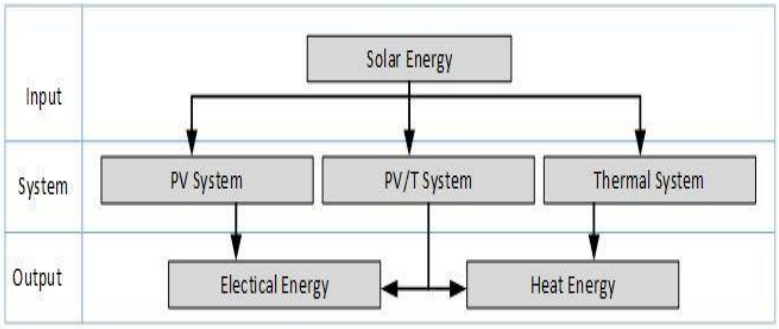

Figure 1. PV system, thermal system, and PV/T system.

Electrical energy and thermal demands are now among the most basic requirements of the structures in which we spend practically all of our time. It is critical, especially in cold areas, to fulfill the electrical energy demand through the same system that meets the high heating energy need. PV/T systems developed for this purpose have two different application types: the roof type and the type integrated into the building. The PV/T systems integrated into the building are mostly used for space heating and are integrated into the building's south, southwest, and west-facing façades, providing an effective solution throughout the day. In this system, the air in the space is used as a fluid, and the need is met by passing it through the PV/T system and returning it directly to the environment. In fact, this system, which acts as an air collector, behaves like a cogeneration system by producing electricity in addition to hot air.

Solar air collectors are generally defined in four different ways: pre-pass, post-pass, double-pass, and matrix pass, depending on the direction of airflow and the location of the flow on the absorber surface (Figure 2).

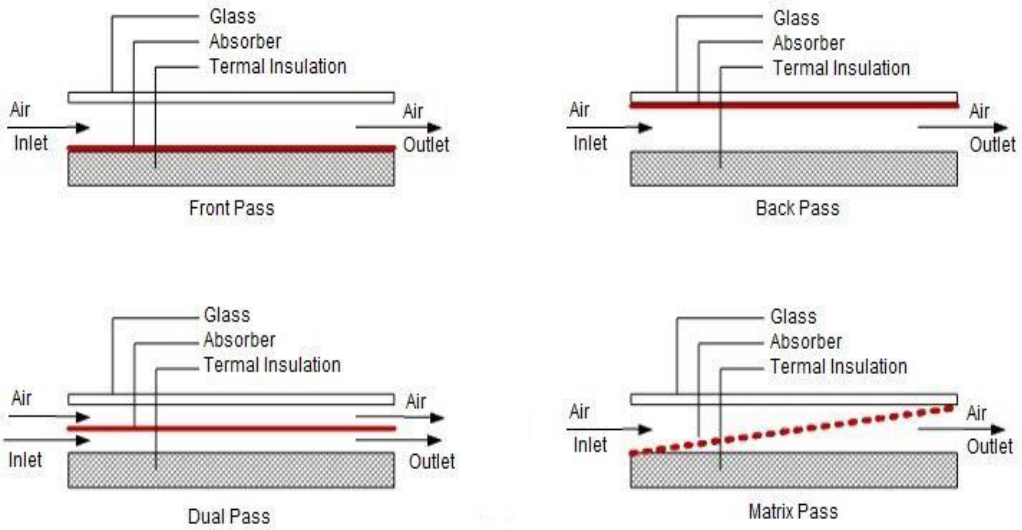

Figure 2. Flow types in air collectors.

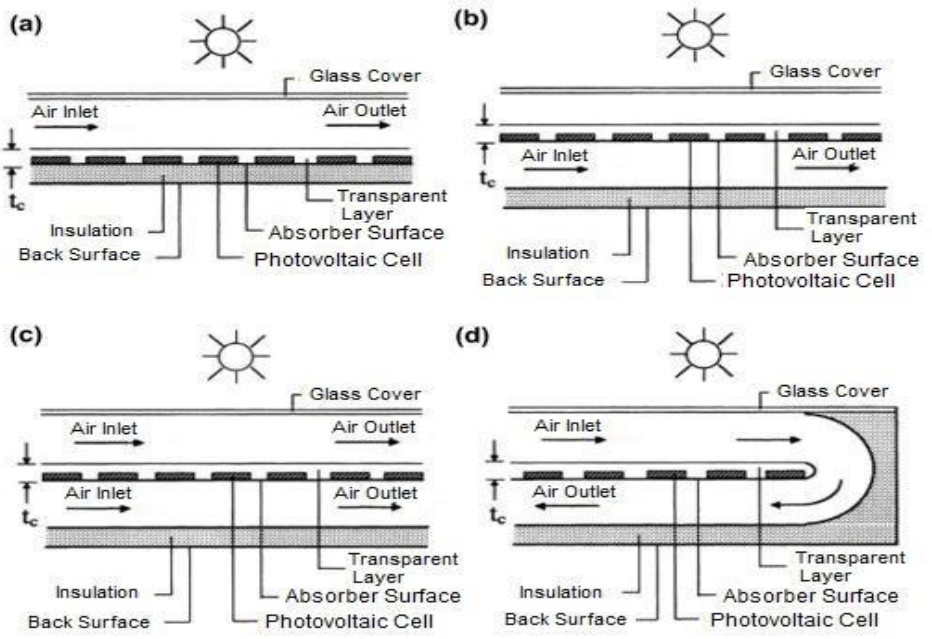

Figure 3. Schematic view of PV/T air collector types [19].

The key elements influencing system efficiency are the location of the flow channel, the velocity of the fluid, and the pressure loss in the flow channel. As a result, while constructing the system, it is critical to design the collector in such a manner that it produces little pressure loss while ensuring maximum flow rate. The most important element influencing the change in the efficiency of solar modules is the temperature of the module's rear surface and the air movement created on this surface. As is well known, some of the solar radiation that reaches the surface of the photovoltaic module is converted into electrical energy, while the remainder is expelled as heat. If a method to lower the rear surface temperature of the solar module is developed, the whole performance of the photovoltaic module will improve. The cross-sections and flow channels of PV/T air collectors designed for this purpose and published in the literature are depicted in Figure 3 [20].

The aim of this study is to determine its performance under the climatic conditions of İzmir province by designing an air source PV/T collector to heat the spaces and meet the partial electricity need, in light of the above information. For this purpose, the design, theoretical analysis, and experimental studies of the system, which are clearly explained in the Method section, were made, and its performance in the winter months was evaluated.

2. Methodology

2.1. Design of PV/T Air Collector

The basic components of the solar-powered air PV/T collector, whose design, application, theoretical, and experimental evaluation were carried out within the scope of this study, consist of a photovoltaic module and solar air collector. The characteristics of the photovoltaic module used in the design of the PV/T air collector are given in Table 1. The photovoltaic module consists of 60 monocrystalline cells, with a peak power of 285 Wp and a module efficiency of 18.2%.

Table 1. Characteristic properties of the PV module.

Nominal Power P_n	Flash Power P_{flash}	Nominal Voltage V_{MPP}	Nominal Current I_{MPP}	Open Circut Voltage V_{oc}	Shortcut Current I_{sc}	Application Class
285 W_p	287 W_p	32,7 V	8,92 A	40,2 V	9,35 A	A Class

The PV/T air collector utilized in the investigation had the following characteristics: The air duct in the PV/T air collector is constructed as a post-pass and has a width of 5 cm. In addition, it is aimed at reducing heat losses and having a smooth

(laminar) flow on the back surface of the air duct by using aluminum foil-coated heat insulation material.

Figure 4 depicts the horizontal section of the designed PV/T air collector, whereas Figure 5 depicts the vertical section. The dimensions in the figures are in cm. The dimensions of the PV/T air collector were established based on the photovoltaic module selected, as shown in the cross-sectional details below.

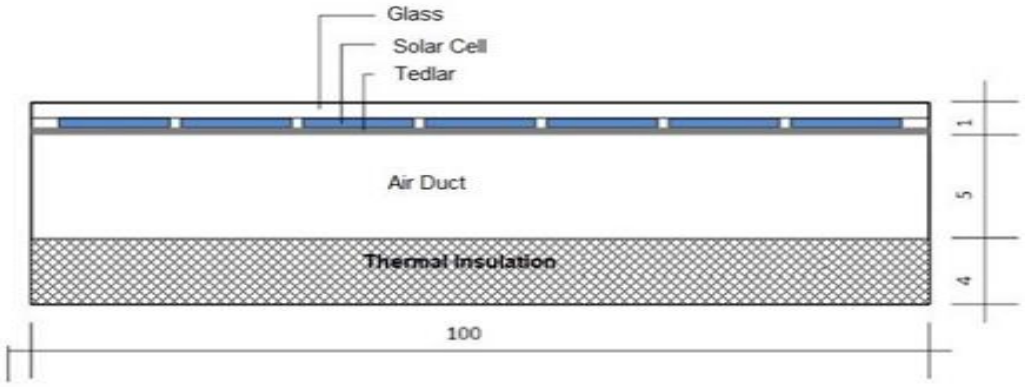

Figure 4. Horizontal section of PV/T air collector.

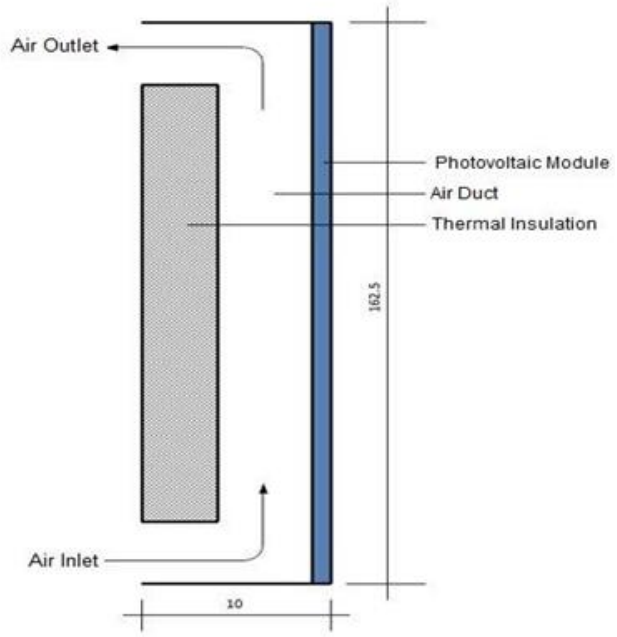

Figure 5. Vertical section of PV/T air collector.

2.2. Theoretical and Experimental Evaluation

The energy balance of the system must be designed in detail in order to determine the theoretical and experimental performance of the PV/T air collector under the climatic conditions of Izmir. Three alternative heat transfer processes are considered when determining the energy balance of the PV/T air collector system (Figures 6 and 7). The thermal study of the PV/T air collector was carried out using the theoretical equations listed below. The heat transfer between the layers of the PV/T air collector is the basis for these equations. When developing the theoretical equations, the following assumptions were made:

- The PV/T air collector system has one-dimensional heat transmission between its layers.
- There is no heat transmission from the PV/T air collector system's edges.
- The materials used to construct the PV/T air collector system have physical and optical qualities that are temperature-independent.

- The contact surfaces of the layers of the PV/T air collection system are all at the same temperature.
- Given the electrical analogy, the heat balance and energy balance equations for different components of the PV/T air collector are shown in Figures 6 and 7.

The energy balance for the solar panel's glass surface can be stated as,

$$m_g C_{p,g} \frac{dT_g}{dt} = q_g(t) - h_{rad,g} A_g (T_g - T_s) - h_{conv,g} A_g (T_g - T_a) - \frac{\lambda_g}{L_g} A_g (T_g - T_c) \quad (1)$$

In this equation, hrad,g expresses the heat transfer from the glass surface of the solar panel to the sky by radiation and is calculated with the help of equation 2, whereas hconv,g denotes heat transfer by convection between the photovoltaic panel's glass surface and the surrounding medium. Furthermore, the quantity qg(t), which is also included in the equation, denotes the amount of solar energy absorbed by the photovoltaic panel's glass and may be determined using equation (3).

$$h_{rad,g} = \frac{\varepsilon \sigma (T_g^4 - T_{sky}^4)}{T_g - T_a} \quad (2)$$

$$q_g(t) = \alpha_g I_\beta(t) A_g \quad (3)$$

The photovoltaic cell's energy balance is as follows,

$$m_c C_{p,c} \frac{dT_c}{dt} = q_c(t) - \frac{\lambda_c}{L_c} A_c (T_c - T_{ted}) - \frac{\lambda_g}{L_g} A_c (T_c - T_g) \quad (4)$$

The term qc(t) in equation (4) relates to the amount of solar energy received by the photovoltaic cell and may be computed using equation (5).

$$q_c(t) = \tau_c \alpha_c (1 - \eta_{PV}) I_\beta(t) A_c \quad (5)$$

The term ηPV in equation (4) refers to the efficiency of a photovoltaic cell as a function of cell temperature and may be computed using equation (6) [21].

$$\eta_{PV} = \eta_{ref} [1 - 0.0054 (T_c - T_{ref})] \quad (6)$$

In this equation, ηref refers to the photovoltaic cell's reference efficiency under 1000 W/m² of radiation, and Tref refers to the cell's reference temperature, which is 25°C as the standard value. The tedlar layer's energy balance is as follows,

$$m_{ted} C_{p,ted} \frac{dT_{ted}}{dt} = -\frac{\lambda_{ted}}{L_{ted}} A_{ted} (T_{ted} - T_c) - h_{rad,ted} A_{ted} (T_{ted} - T_{ins,1}) - h_{conv,ted} A_{ted} (T_{ted} - T_f) \quad (7)$$

The flow channel's energy balance is as follows,

$$m_f C_{p,f} \frac{dT_f}{dt} = -\dot{m} C_{p,f} (T_{f,out} - T_{f,in}) - h_{conv,ted} A_{ted} (T_f - T_{ted}) - h_{conv,ins} A_{ins} (T_f - T_{ins,1}) \quad (8)$$

T_f in this equation represents the average temperature in the flow channel and is calculated by means of equation (9).

$$T_f = \frac{T_{f,in} + T_{f,out}}{2} \quad (9)$$

The insulating layer's energy balance is as follows,

$$m_{ins} C_{p,ins} \frac{dT_{ins}}{dt} = -\frac{\lambda_{ins}}{L_{ins}} A_{ins} (T_{ins,1} - T_{ins,2}) - h_{conv,ins} A_{ins} (T_{ins,1} - T_f) - h_{conv,ins} A_{ins} (T_{ins,2} - T_r) \quad (10)$$

The total heat loss coefficient (UT) is a collector property that has a direct impact on its performance. This coefficient is used to calculate the collector's performance, the quantity of usable heat it creates, and the collector's efficiency. The total heat loss coefficient is determined as the inverse of the thermal resistance using the following equation:

$$U_T = U_t + U_b \quad (11)$$

Ut in this equation shows the heat loss coefficient of the photovoltaic panel, the top layer forming the PV/T collector, and is calculated by means of the equation (12). Ub is the heat loss coefficient in the thermal insulation material, which is the substrate of the PV/T collector, and is calculated by means of equation (13).

$$U_t = \frac{1}{\frac{1}{h_{rad,g} + h_{conv,g}} + \frac{\lambda_g}{L_g} + \frac{\lambda_c}{L_c} + \frac{\lambda_{ted}}{L_{ted}}} \quad (12)$$

$$U_b = \frac{1}{\frac{1}{h_{rad,ins}+h_{conv,ins}}+\frac{\lambda_{ins}}{L_{ins}}} \quad (13)$$

The useful heat to be obtained from the PV/T collector is expressed as follows, depending on the inlet, the outflow temperature, and the flow rate of air in the flow channel.

$$Q_u = \dot{m}C_{p,f}\left(T_{f,out} - T_{f,in}\right) \quad (14)$$

The useful heat of the PV/T collector is expressed as indicated in equation (14), based on the total heat flux.

$$Q_u = \left[\left(\tau_g \alpha_c \tau_{ted} I_\beta A_c\right) - U_T A_c (T_{ted} - T_a)\right] \quad (15)$$

The thermal efficiency of the PV/T collector is calculated as expressed in equation (16).

$$\eta_{th} = \frac{Q_u}{A_c I_\beta} = \frac{\dot{m}C_{p,f}\left(T_{f,out}-T_{f,in}\right)}{A_c I_\beta} \quad (16)$$

In other words, the thermal efficiency of the collector can also be calculated using the following equation.

$$\eta_{th} = \frac{Q_u}{A_c I_\beta} = \frac{\left[\left(\tau_g \alpha_c \tau_{ted} I_\beta A_c\right) - U_T A_c (T_f - T_a)\right]}{A_c I_\beta} = \tau_g \alpha_c \tau_{ted} - \frac{U_T\left(T_{f,out}-T_{f,in}\right)}{I_\beta} \quad (17)$$

The total efficiency of the PV/T totalizer is determined as follows considering the equation (6) and equation (16, 17).

$$\eta = \eta_{th} + \eta_{PV} \quad (18)$$

An iterative technique was employed in the numerical computation with the help of the preceding equations to find the temperature-dependent impacts of the heat transfer coefficient. Temperatures for each layer of the PV/T collector were calculated using Excel-based software and the fourth-order Runga-Kutta method. Table (2) details the accepted physical and thermal parameters of the PV/T collector during these calculations.

Table 2. Physical and thermal properties of the PV/T air collector.

Parameters	Properties	Unit	Parameters	Properties	Unit
A_{PV}	1,6012	m²	σ	5,671 10^{-8}	J/m²sK⁴
A_g	1,6012	m²	$C_{p,g}$	840	J/kgK
A_c	1,4415	m²	$C_{p,c}$	700	J/kgK
A_{ted}	1,6012	m²	$C_{p,ted}$	560	J/kgK
A_{ins}	1,5212	m²	$C_{p,ins}$	880	J/kgK
τ_g	0,90	-	ε_g	0,88	-
τ_{ted}	0,92	-	ε_c	0,35	-
α_g	0,05	-	ε_{ted}	0,95	-
α_c	0,95	-	ε_{ins}	0,05	-
λ_g	1,10	W/mK	ρ_g	2700	kg/m³
λ_c	130	W/mK	ρ_c	2330	kg/m³
λ_{ted}	0,033	W/mK	ρ_{ted}	1200	kg/m³
λ_{ins}	0,040	W/mK	ρ_{ins}	15	kg/m³

There are many experimental studies in the literature developed to determine the experimental performance of PV/T systems [22]–[24]. However, since each study has its own unique setup, a unique experimental setup was created within the scope of this study. The experimental setup formed is shown in Figure 8, the placement of the devices used is given in Figure 9, and the technical features are given in Table 3. According to Figure 9, the measuring points and measuring sensors are as follows:

- Point 1, Solar Radiation (W/m²),
- Point 2, Ambient Temperature (°C) and Humidity (%),
- Point 3, the inlet Temperature (°C) of the PV/T Collector,
- Point 4, the outflow Temperature (°C) of the PV/T Collector,
- Point 5, Room Temperature (°C) and Humidity (%),
- Point 6, Middle Point Temperature (°C) of the Room,
- Point 7, PV panel Current (A), Voltage (V), front and back surface Temperature (°C)

Table 3. Measuring device and sensors.

Main Section	Usage	Specification/description
Sensors	Solar sensor	Type: CMP 11 Pyranometer, Sensivity: ±1% (between -10°C and +40°C), Response time: 12s (between -40°C and +80°C)
	Temperature and Humidity sensor	Type: CS 215 Humidity and Temperature Sensor, Relative Humidity: Measurement Range: 0 to 100%, Error Limit: < 3% Temperature Measurement Range: -40°C to 56°C, Error Limit: <0,5°C
	Temperature sensor	Type: Model 107 , Measurement Range: -40°C to 56°C, Error Limit: <0,5°C
Data-Logger Unit	Use for data storage	Type CR1000 Campbell Data-Logger Capacity: 6MB SRAM, Channels: 16 single-ended or 8 differential,
Electricity Power		The voltage produced: 15,1 V, Peak power: 10 W

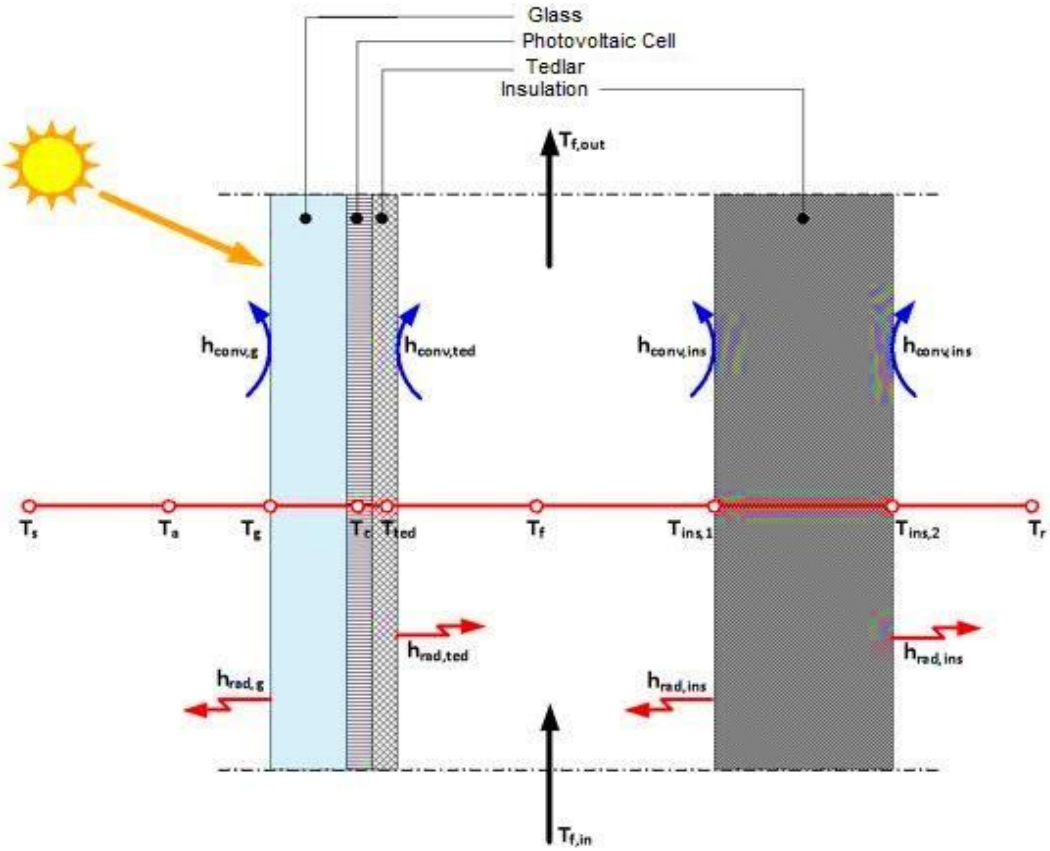

Figure 6. Heat transfer of PV/T air collector.

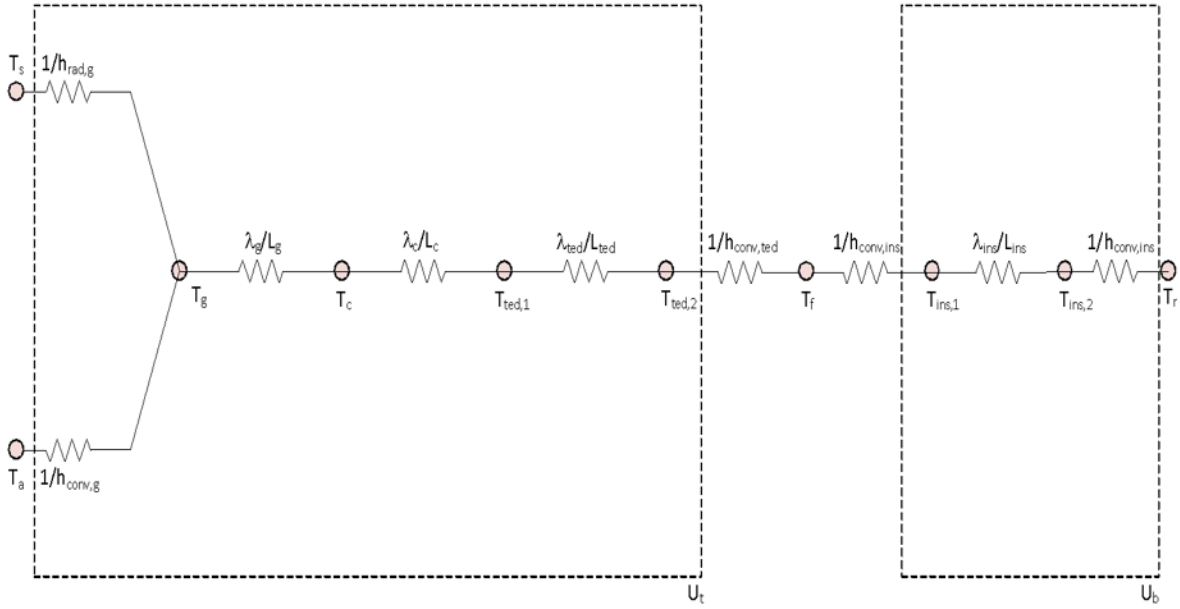

Figure 7. Equivalent circuit diagram of the PV/T air collector.

Figure 8. Mounted view of PV/T air collector.

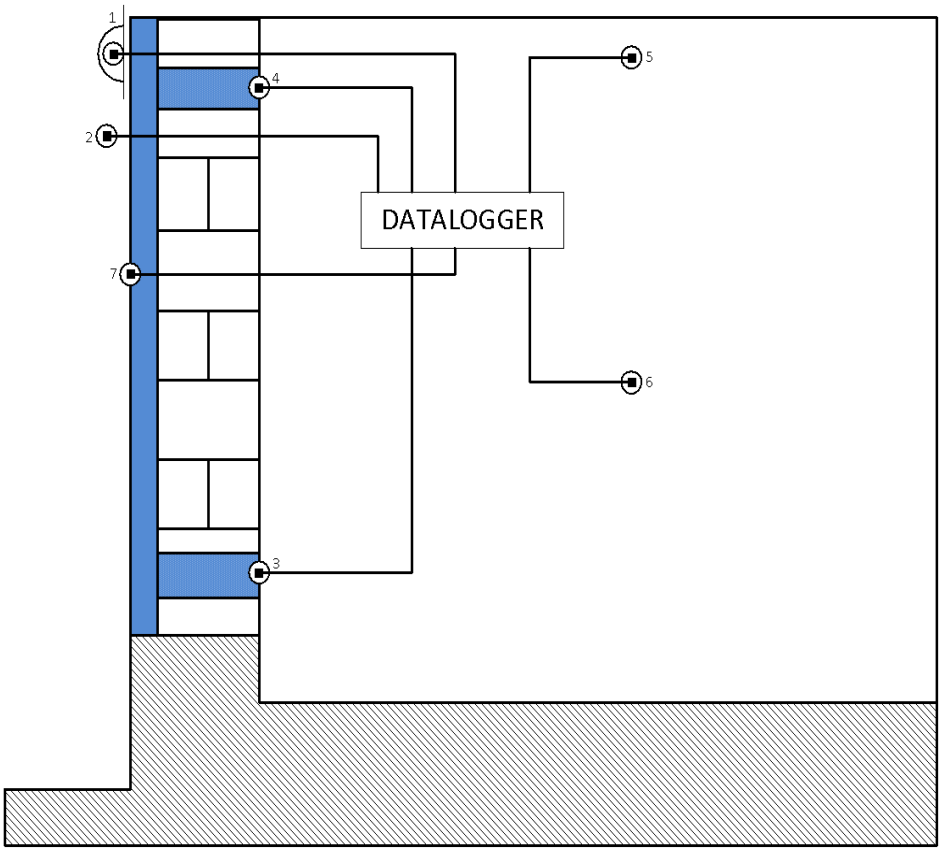

Figure 9. Measuring points in the experimental setup.

3. Analysis and Results

3.1. Analysis

To determine the performance of the designed PV/T solar air collector under İzmir environmental conditions, evaluations were done using data collected from the calculation method and experimental setup. In the experimental studies carried out in December, January, and February, the periodic change of solar radiation from external factors is given in Figure 10, and the change of outdoor temperature and outdoor humidity is shown in Figure 11.

.

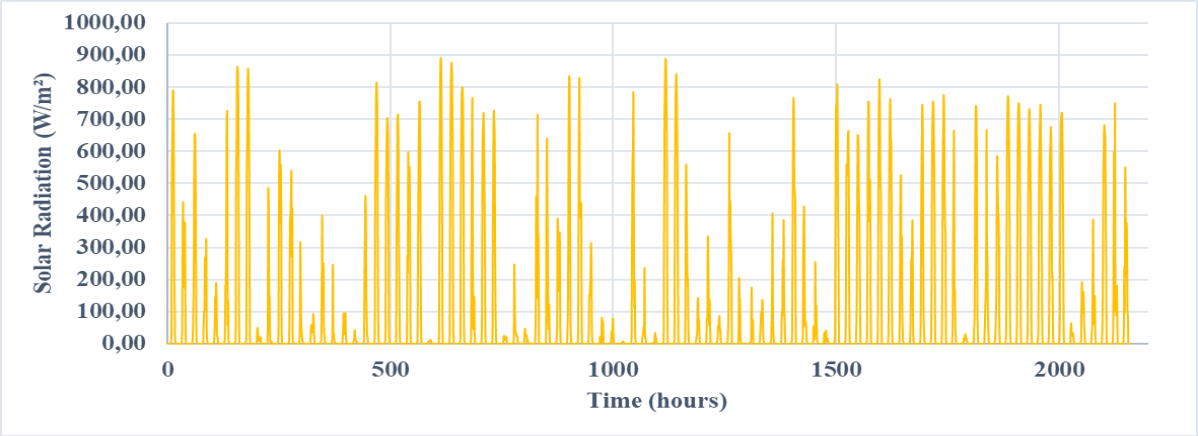

Figure 10. Global solar radiation between December to February.

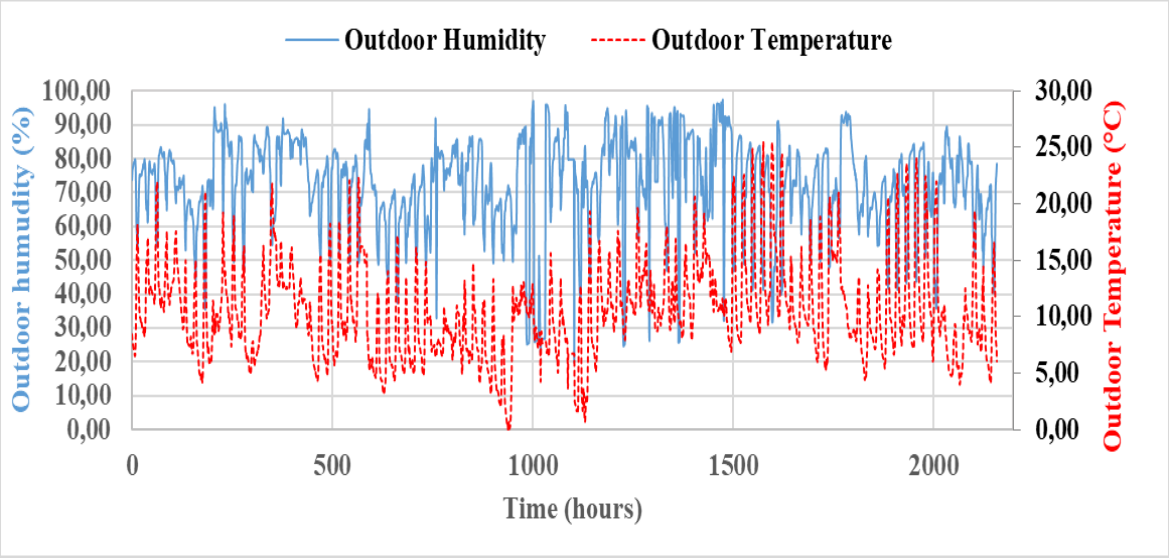

Figure 11. Ambient temperature and relative humidity between December to February.

As a result of the experimental studies performed to determine the performance of the PV/T solar air collector in the winter climatic conditions of Izmir, the results obtained for the average days given in Table 4 are shown in Figure 12.

Table 4. Recommended average days of months (Duffie and Beckman (2013)).

Months	Day of month	For the average day of the month		
		Day	n	δ (°)
January	i	17	17	-20,9
February	31+i	16	47	-13,0
March	59+i	16	75	-2,4
April	90+i	15	105	9,4
May	120+i	15	132	18,8
June	151+i	11	162	23,1
July	181+i	17	198	21,2
August	212+i	16	228	13,5
September	243+i	15	258	2,2
October	273+i	15	288	-9,6
November	304+i	14	318	-18,9
December	334+i	10	344	-23,0

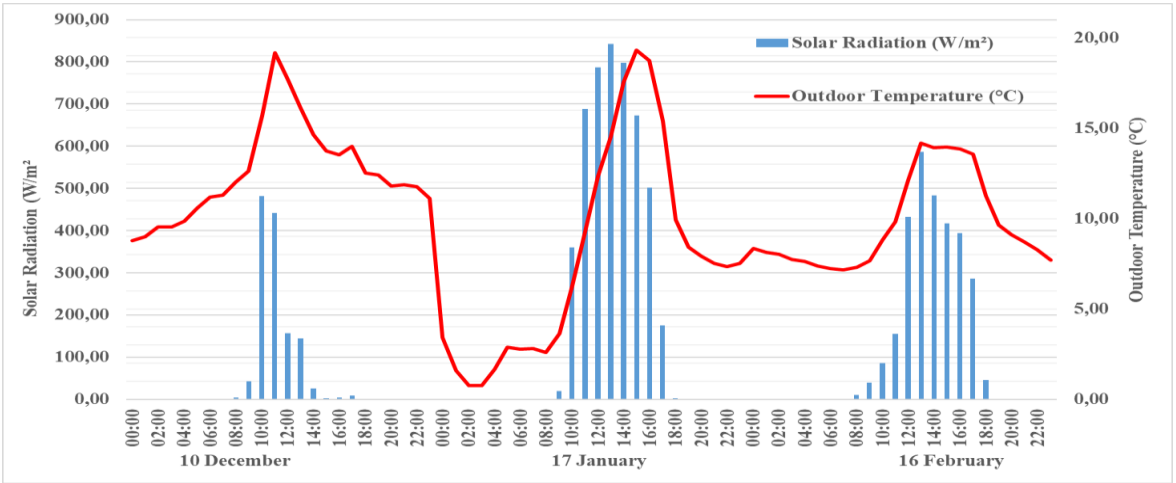

Figure 12. Hourly variation of solar radiation and ambient temperature.

3.2 Results

days mentioned above, the findings obtained from the system are given in detail below. In experimental studies, the system was operated with natural airflow. The findings described in Table 4 for the day representing each month between December and February are given in between Figure 13 and Figure 17.

As a result of the experimental studies carried out during the

In accordance with the experimental studies conducted on December 10th, whose temperature variations are shown in Figure 13, the outdoor temperature change's amplitude is 10.39 °C, while the indoor temperature change's amplitude is 1.60 °C. At the same time, the highest temperature differential between the PV/T collector's inlet and its outflow was 7.87 °C.

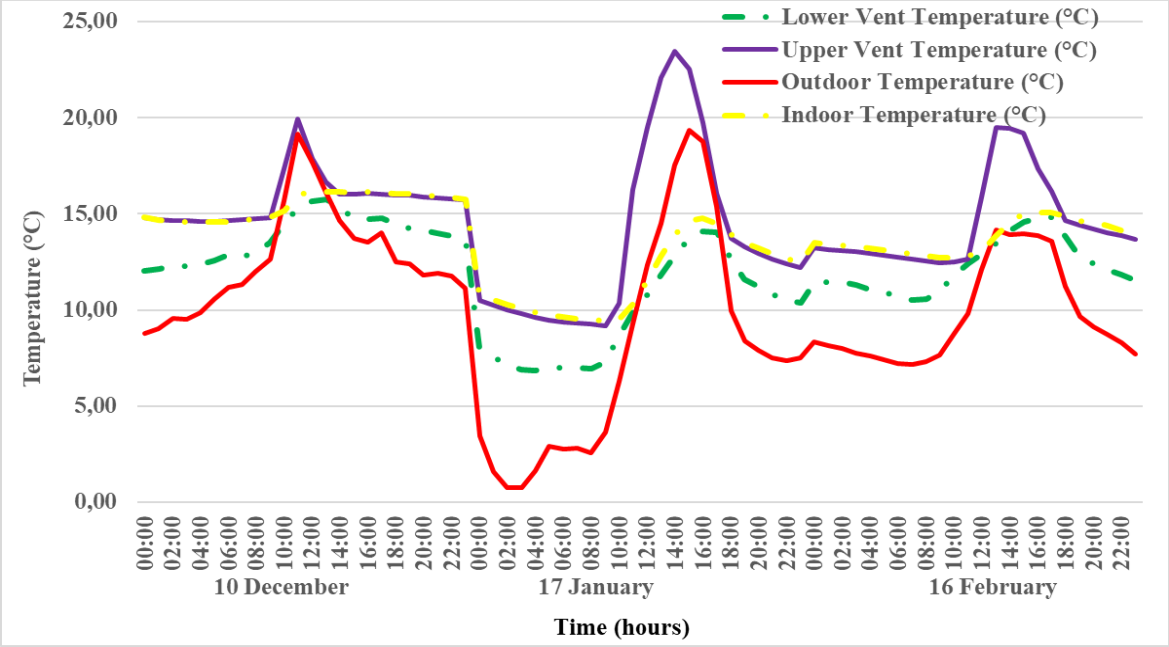

Figure 13. Hourly variation of indoor-outdoor and PV/T collector input-output temperature.

According to experimental studies conducted on January 17, which corresponds to the month of January, the PV/T collector, the inlet and outflow temperatures, and the hourly variation of the outdoor and indoor environments are shown in Figure 13.

Figure 13 indicates that the external temperature change had an amplitude of 18.57 °C and the internal temperature change had an amplitude of 5.35 °C. At the same time, the maximum difference between the inlet and the outflow temperatures of the PV/T collector was 16.59 °C.

The hourly change of the outside and indoor environments, as well as the PV/T collector's inlet and outflow temperatures, are illustrated in Figure 13 in accordance with the experimental studies conducted on February 16, which serves as a representation of the month of February. During the day, the amplitude of the outdoor temperature change was 7.02 °C, while the amplitude of the indoor temperature change was 2.35 °C. At the same time, the difference between the inlet and the outflow temperatures of the PV/T collector was realized to be 8.96 °C.

The change in electrical efficiency obtained from the panel depending on the temperature values formed on the back surface is shown in Figure 14. On December 10, the front surface of the PV panel was observed to rise to a maximum of 26.98 °C, depending on the density of solar radiation, and a minimum of 25.24 °C on the back surface.

Figure 14 illustrates the temperature difference of the PV panel's front and back surfaces on January 17. On the front surface of the PV panel, the temperature increase reached its peak at 43.47 °C, while it was 37.69 °C on the back.

The front and back surface temperatures of the PV panel changed throughout the day of February 16, as shown in Figure 14. The PV panel's front surface experienced a maximum increase of

32,73 °C, while its back surface experienced a maximum increase of 29,42 °C.

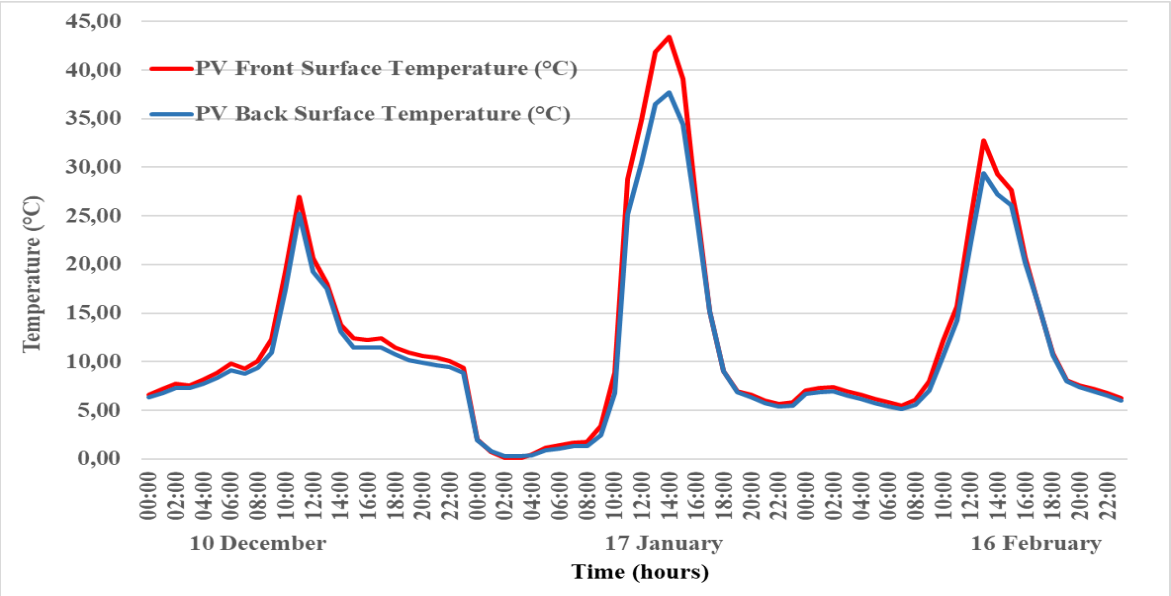

Figure 14. Hourly variation of front and back surface temperature of the PV panel.

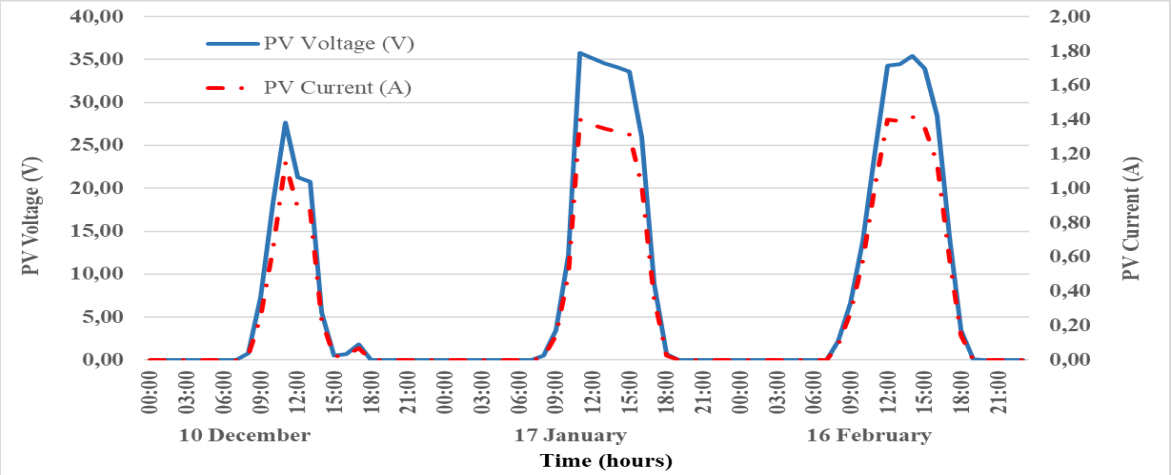

Figure 15. Hourly variation of voltage and current of the PV panel.

As demonstrated in Figure 15, the maximum PV produced on December 10 was 38.94 V, and the current generated was 1.62 A. These results indicate that the PV panel's maximum power of 62.89 W was obtained. Under typical test conditions, the power generated by PV is far less than 285 W. This is due to the vertical orientation of the PV panel. The PV panel's maximum voltage on January 17 was 36.17 V, and the maximum current it could produce was 1.45 A. These results indicate that PV produced a maximum power of 52.30 W. The highest PV value produced during the day on February 16 was 38.48 V, while the current value it produced was 1,61 A. According to these values, the maximum power of 62.03 W was obtained from PV.

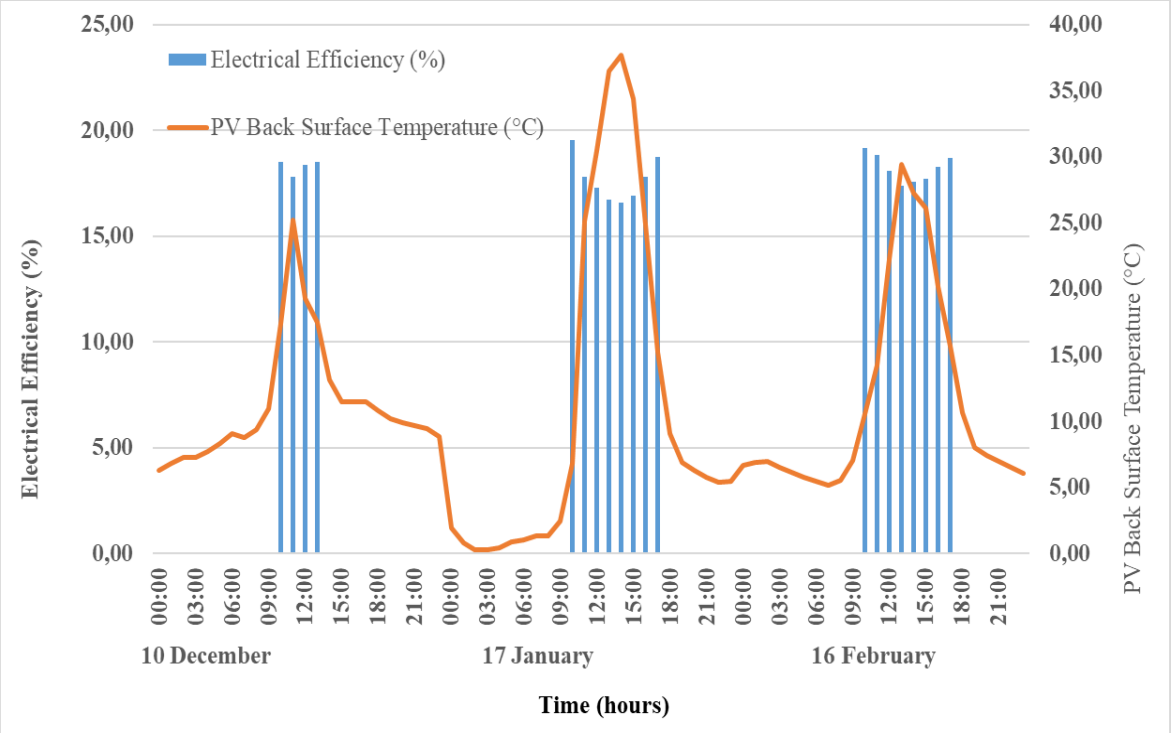

Figure 16. Hourly variation of back surface temperature and electrical efficiency of the PV panel.

According to the temperature values produced on the PV panel's back surface, the electrical efficiency of the panel changes, as illustrated in Figure 16.

The lowest and maximum electrical efficiencies predicted based on the back surface temperature of the PV panel were 17.78% and 18.53, respectively, according to tests taken on December 10. The efficiency of the PV panel is roughly 1.65%, while considering that the project's PV panel has an efficiency of 18.2% under typical test settings. This is because the temperature change behind the PV panel in summer is higher than the standard test temperature of 25 °C.

According to the values obtained on January 17, the calculated lowest electrical efficiency obtained from the PV panel is 16.58%, while the highest is 19.55%, depending on the back surface temperature of the PV panel. According to the yield value of the PV panel under standard test conditions, it has an average yield reduction of around 1.85%.

According to the values obtained on February 16, depending on the back surface temperature of the PV panel during the day, the electrical efficiency obtained from the PV panel was calculated as the lowest (17.38%) and the highest (19.18%). According to the yield value of the PV panel under standard test conditions, the efficiency of the PV panel is approximately 1.59%.

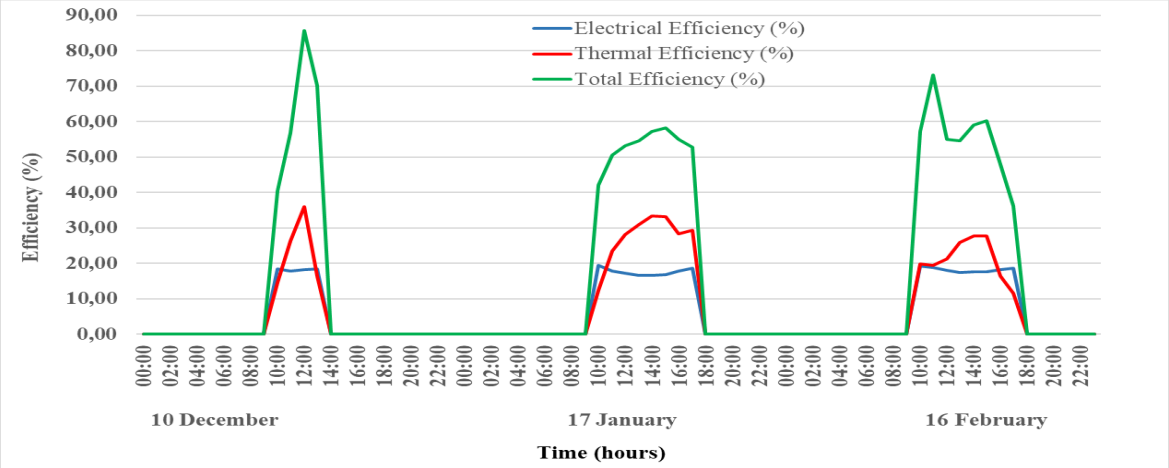

Figure 17. Hourly variation of electrical, thermal and total efficiency of the PV/T collector.

The electrical, thermal, and overall efficiency change of the system was computed in accordance with the results of the experimental study carried out on December 10, January 17, and February 16 and is shown in Figure 17.

The results of the experimental investigation conducted on December 10 showed that, depending on the hourly solar radiation value, the system's thermal efficiency ranged from 14,64% to 35,94%, with 14,64% being the lowest and 35,94% being the greatest. The fluid entering the collector had a temperature range of 12,06 °C to 15,73 °C, which was used to calculate the PV/T collector's change in thermal efficiency. The results of the experimental investigation conducted on January 17 indicated that, depending on the hourly solar radiation value, the system's lowest thermal efficiency was 12,45% and its greatest was 33,39%. The fluid entering the PV/T collector had a temperature value of 6,84 °C when the lowest thermal efficiency change was calculated, and 14,09 °C when the highest. The results of the experimental investigation conducted on February 16 indicated that the system's thermal efficiency ranged from 3,78% to 27,78%, depending on the value of the hourly solar radiation.

The verification method used to compare the results obtained in light of the experimental and theoretical studies carried out within the scope of this study is Root Mean Square Error (RMSE). The equation used in the determination of error analysis is as follows;

$$RMSE = \sqrt{\frac{1}{n}\sum_{i=1}^{n}\left(x_{theo,i} - x_{exp,i}\right)^2} \quad (18)$$

The results of the error analysis performed in light of the data obtained from the experimental and theoretical studies are given in Table 5. Error values calculated depending on ambient conditions are given for PV cell temperature, fluid temperature, thermal, electrical, and total efficiency. According to the error evaluation revealed as a result of the theoretical and experimental studies, the average error rates were calculated as 4.19% according to the PV cell temperature, 5.00% according to the fluid temperature, 0.07% according to the thermal efficiency, 0.03% according to the electrical efficiency, and 0.04% according to the total efficiency.

Table 5. Percentage errors between theoretical and experimental results.

T_a	I_β	Root Mean Square Error (RMSE) (%)				
(K)	(W/m^2)	T_c	T_f	η_{th}	η_{pv}	η
275-280	600-700	3.99	4.56	0.12	0.02	0.04
280-285	200-300	6.06	2.34	0.11	0.03	0.05
	700-800	4.65	4.88	0.08	0.03	0.04
	800-900	4.02	6.76	0.05	0.02	0.03
285-290	400-500	3.23	3.13	0.10	0.04	0.04
	500-600	3.05	3.98	0.07	0.03	0.05

	600-700	2.99	4.12	0.06	0.02	0.03
	700-800	2.76	5.05	0.05	0.02	0.03
	800-900	2.89	7.79	0.04	0.02	0.03
	600-700	4.76	4.22	0.06	0.03	0.04
290-300	700-800	5.18	5.15	0.05	0.03	0.04
	800-900	6.66	8.02	0.04	0.02	0.03
Average		**4.19**	**5.00**	**0.07**	**0.03**	**0.04**

4. Conclusion

The benefit of the PV/T collector system, which serves as the project's foundation, is that the heat created by the PV panel is transported to the air gap established behind the PV panel, allowing the PV module to cool and therefore boost its electrical efficiency. The potential heat generation at the given surface is substantially greater than the electrical performance. In order to ensure the use of PV panels and thermal solar collectors together, it will be more appropriate to use materials that perform heat transfer faster. For this, instead of TEDLER, which is used as a back surface element in traditional photovoltaic panels, the use of materials with high heat transfer coefficients, such as copper or aluminum, will directly contribute to the increase in system performance. PV requires a low temperature for high efficiency; the air solar collector requires a high temperature to produce a high benefit. Current technologies have lower efficiency than 2 separate systems in PV/T collectors, and also because of the initial development step, the PV/T combination is more expensive. However, it is still considered advantageous in terms of aesthetics, future cost reductions (production and installation), and market and consumer needs.

Türkiye, with an average yearly solar energy of 1311 kWh/m² year and a total annual sunlight duration of 2640 hours, is a fortunate country in terms of solar energy potential. If the existing potential is evaluated, the dependence on external energy will be greatly reduced, but the initial installation costs of solar power systems are often quite high. The production of electricity with solar cells is not yet used because it is expensive. The widespread use of electricity, as well as hot water from solar energy in buildings, will significantly reduce environmental pollution. Despite the system's high initial investment cost, its long-term benefit to the national economy and environment will be beneficial. Using these two transducers together reduces costs while increasing system productivity and utilization.

The housing sector consumes 34% of total energy. On a sectoral basis, housing has a large share of energy consumption. In this context, efforts to reduce energy consumption in houses will contribute to the national economy, and at the same time, reduce environmental problems related to fossil fuel consumption.

For this, it is possible to create effective solutions by integrating photovoltaic panels with air solar energy collectors used for heating the spaces. As a result of the studies carried out to determine the experimental performance of the PV/T air collector developed within the scope of the study, the thermal efficiency of the system reached up to 35% and the electrical efficiency reached 19% during the winter months. As a result of comparing the results obtained from theoretical and experimental studies, it has been determined that there is an error of 0.12%.

Acknowledgment

This work was supported by Research Fund of the Dokuz Eylul University. Project Number: 2017.KB.FEN.009

Contributions of the Authors

All authors contributed equally to the study.

Conflict of Interest Statement

There is no conflict of interest between the authors.

Statement of Research and Publication Ethics

The study is complied with research and publication ethics

References

[1] S. C. Solanki, S. Dubey, and A. Tiwari, "Indoor simulation and testing of photovoltaic thermal (PV/T) air collectors," *Appl Energy*, vol. 86, no. 11, pp. 2421–2428, Nov. 2009, doi: 10.1016/J.APENERGY.2009.03.013.

[2] S. R. Reddy, M. A. Ebadian, and C. X. Lin, "A review of PV–T systems: Thermal management and efficiency with single phase cooling," *Int J Heat Mass Transf*, vol. 91, pp. 861–871, Dec. 2015, doi: 10.1016/J.IJHEATMASSTRANSFER.2015.07.134.

[3] A. N. Al-Shamani, K. Sopian, S. Mat, H. A. Hasan, A. M. Abed, and M. H. Ruslan, "Experimental studies of rectangular tube absorber photovoltaic thermal collector with various types of nanofluids under the tropical climate conditions," *Energy Convers Manag*, vol. 124, pp. 528–542, Sep. 2016, doi: 10.1016/J.ENCONMAN.2016.07.052.

[4] C. Babu and P. Ponnambalam, "The role of thermoelectric generators in the hybrid PV/T systems: A review," *Energy Convers Manag*, vol. 151, pp. 368–385, Nov. 2017, doi: 10.1016/J.ENCONMAN.2017.08.060.

[5] A. Makki, S. Omer, and H. Sabir, "Advancements in hybrid photovoltaic systems for enhanced solar cells performance," *Renewable and Sustainable Energy Reviews*, vol. 41, pp. 658–684, Jan. 2015, doi: 10.1016/J.RSER.2014.08.069.

[6] Ömeroğlu G, "Fotovoltaik - Termal (PV / T) Sistemin Sayısal (CFD) ve Deneysel Analizi," *Fırat Üniversitesi Mühendislik Bilimleri Dergisi*, vol. 30, no. 1, pp. 161–167, Mar. 2018.

[7] I. Nardi, D. Ambrosini, T. de Rubeis, D. Paoletti, M. Muttillo, and S. Sfarra, "Energetic performance analysis of a commercial water-based photovoltaic thermal system (PV/T) under summer conditions," *J Phys Conf Ser*, vol. 923, p. 012040, Nov. 2017, doi: 10.1088/1742-6596/923/1/012040.

[8] A. Shukla, K. Kant, A. Sharma, and P. H. Biwole, "Cooling methodologies of photovoltaic module for enhancing electrical efficiency: A review," *Solar Energy Materials and Solar Cells*, vol. 160, pp. 275–286, Feb. 2017, doi: 10.1016/J.SOLMAT.2016.10.047.

[9] P. Xu *et al.*, "A review of thermal absorbers and their integration methods for the combined solar photovoltaic/thermal (PV/T) modules," *Renewable and Sustainable Energy Reviews*, vol. 75, pp. 839–854, Aug. 2017, doi: 10.1016/J.RSER.2016.11.063.

[10] Z. Qiu, X. Ma, X. Zhao, P. Li, and S. Ali, "Experimental investigation of the energy performance of a novel Micro-encapsulated Phase Change Material (MPCM) slurry based PV/T system," *Appl Energy*, vol. 165, pp. 260–271, Mar. 2016, doi: 10.1016/J.APENERGY.2015.11.053.

[11] M. J. Huang, P. C. Eames, and B. Norton, "Phase change materials for limiting temperature rise in building integrated photovoltaics," *Solar Energy*, vol. 80, no. 9, pp. 1121–1130, Sep. 2006, doi: 10.1016/J.SOLENER.2005.10.006.

[12] S. Preet, B. Bhushan, and T. Mahajan, "Experimental investigation of water based photovoltaic/thermal (PV/T) system with and without phase change material (PCM)," *Solar Energy*, vol. 155, pp. 1104–1120, Oct. 2017, doi: 10.1016/J.SOLENER.2017.07.040.

[13] C. S. Malvi, D. W. Dixon-Hardy, and R. Crook, "Energy balance model of combined photovoltaic solar-thermal system incorporating phase change material," *Solar Energy*, vol. 85, no. 7, pp. 1440–1446, Jul. 2011, doi: 10.1016/J.SOLENER.2011.03.027.

[14] Rüstemli S, Dinçer F, Çelik M, and Cengiz M. S, "Fotovoltaik Paneller: Güneş Takip Sistemleri ve İklimlendirme Sistemleri," *Bitlis Eren Üniversitesi Fen Bilimleri Dergisi*, vol. 2, no. 2, pp. 141–147, 2013.

[15] H. M. S. Bahaidarah, "Experimental performance evaluation and modeling of jet impingement cooling for thermal management of photovoltaics," *Solar Energy*, vol. 135, pp. 605–617, Oct. 2016, doi: 10.1016/J.SOLENER.2016.06.015.

[16] H. A. Hasan, K. Sopian, A. H. Jaaz, and A. N. Al-Shamani, "Experimental investigation of jet array nanofluids impingement in photovoltaic/thermal collector," *Solar Energy*, vol. 144, pp. 321–334, Mar. 2017, doi: 10.1016/J.SOLENER.2017.01.036.

[17] S. A. Klein, J. A. Duffie, and W. A. Beckman, "Transient Considerations of Flat-Plate Solar Collectors," *Journal of Engineering for Power*, vol. 96, no. 2, pp. 109–113, Apr. 1974, doi: 10.1115/1.3445757.

[18] A. Suzuki and S. Kitamura, "Combined Photovoltaic and Thermal Hybrid Collector," *Jpn J Appl Phys*, vol. 19, no. S2, p. 79, Jan. 1980, doi: 10.7567/JJAPS.19S2.79.

[19] A. A. Hegazy, "Comparative study of the performances of four photovoltaic/thermal solar air collectors," *Energy Convers Manag*, vol. 41, no. 8, pp. 861–881, May 2000, doi: 10.1016/S0196-8904(99)00136-3.

[20] K. Moradi, M. Ali Ebadian, and C. X. Lin, "A review of PV/T technologies: Effects of control parameters," *Int J Heat Mass Transf*, vol. 64, pp. 483–500, Sep. 2013, doi: 10.1016/J.IJHEATMASSTRANSFER.2013.04.044.

[21] L. M. Candanedo, A. Athienitis, and K.-W. Park, "Convective Heat Transfer Coefficients in a Building-Integrated Photovoltaic/Thermal System," *J Sol Energy Eng*, vol. 133, no. 2, May 2011, doi: 10.1115/1.4003145.

[22] E. Touti, M. Masmali, M. Fterich, and H. Chouikhi, "Experimental and numerical study of the PVT design impact on the electrical and thermal performances," *Case Studies in Thermal Engineering*, vol. 43, 2023, doi: 10.1016/j.csite.2023.102732.

[23] C.-Y. Huang, H.-C. Sung, and K.-L. Yen, "Experimental Study of Photovoltaic/Thermal (PV/T) Hybrid System," *International Journal of Smart Grid and Clean Energy*, vol. 2, no. 2, 2013, doi: 10.12720/sgce.2.2.148-151.

[24] A. Buonomano, F. Calise, and M. Vicidomini, "Design, simulation and experimental investigation of a solar system based on PV panels and PVT collectors," *Energies (Basel)*, vol. 9, no. 7, 2016, doi: 10.3390/en9070497.